Surface Structure of Asymmetric Fluorinated Block Copolymers

Hideaki Yokoyama*

Center of Macromolecular Technology, National Institute of Advanced Industrial Science and Technology, 2-41-6 Aomi, Kotoh-ku, Tokyo 135-0064, Japan

Keiji Tanaka, Atsushi Takahara,† and Tisato Kajiyama

Department of Applied Chemistry, Faculty of Engineering, Kyushu University, Fukuoka 812-8581, Japan

Kenji Sugiyama and Akira Hirao

Department of Polymer Chemistry, Faculty of Engineering, Tokyo Institute of Technology, Ookayama, Tokyo 152-8552, Japan

Received August 13, 2003; Revised Manuscript Received November 6, 2003

ABSTRACT: Surface structures of asymmetric poly[styrene-*block*-4-(perfluorooctylpropyloxy)styrene] block copolymers (PS−PF) with the shorter PF block than the PS block have been investigated using X-ray photoelectron spectroscopy (XPS) and dynamic secondary ion mass spectrometry (SIMS). Fluorooctyl side groups (C_8F_{17}) of the block copolymers segregate to the surface due to their low surface energy. Asymmetry of the block remarkably influences the structure of the C_8F_{17} side groups and the backbone of PS−PF copolymers at the surface. When a weight fraction of the PF block, f_{PF}^{wt}, is 0.09, the surface is partially covered by the C_8F_{17} side groups with a thickness thinner than the length of the C_8F_{17} side group. The C_8F_{17} side groups hence lie parallel to the surface. When f_{PF}^{wt} is approximately 0.25, the backbone of the PF block lies parallel to the surface, and the C_8F_{17} side groups stand perpendicular to the surface. Such a conformation results in a domain thickness of the PF block comparable to the length of the C_8F_{17} side group. However, as f_{PF}^{wt} goes beyond 0.3, the backbone of the PF block orients toward the surface while the top surface region, i.e., 1.5 nm from the surface, is still occupied by the C_8F_{17} side groups standing perpendicular to the surface.

Introduction

Fluorinated polymers provide low surface energy materials widely applicable for industrial applications, such as coatings and nonwetting biological applications.[1−4] On the other hand, fluorinated polymers are difficult to use due to poor solubility and processability. It has been revealed experimentally that a fluorinated block of fluorinated block copolymers segregates to the surface.[5,6] Therefore, fluorinated block copolymers potentially cover the surface with a limited fluorinated block fraction while maintaining solubility in ordinary solvents and processability.

It is well-known theoretically and experimentally that a bulk structure of block copolymers is determined by a function of the volume fraction, f, and χN, where χ is the interaction parameter between monomers of two consisting blocks and N is the total number of monomers.[7,8] Depending on f and χN, block copolymers show a variety of ordered structures in bulk such as spheres, cylinders, gyroids, and lamellae. However, at the surface, the difference in surface energies of blocks, $\Delta\gamma$, gives an additional restriction for a block copolymer to adopt a structure, resulting in a surface domain structure different from that in bulk. For instance, lamellae seem to adopt planar restriction and a surface energy requirement by selectively placing the lower energy block domain at the surface and forming parallel layers, but spheres or cylinders in which the shorter blocks have the lower surface energy have difficulties to overcome the restriction. Surface and bulk structures of block copolymers are schematically shown in Figure 1. When the block with the lower surface energy adopts a lamella or a continuous domain as in Figure 1C,D, the surface domain structures have almost no difference from their bulk structures. When the block with the lower surface energy forms discrete domains such as the spheres or the cylinders in Figure 1B or a block copolymer is in a disordered phase in bulk as schematically shown in Figure 1A, their surface domain structures are very different from the naturally adopted structures in bulk. When a block copolymer with high asymmetry has to form half of a lamella at the surface as in Figure 1A,B, the longer block with higher surface energy has to be

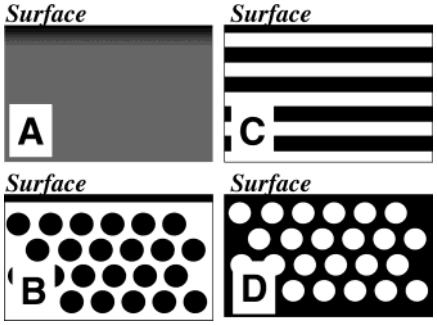

Figure 1. Schematic pictures of domain structures near the surface. The black domains are those of the lower surface energy block which tends to segregate to the surface. (A) A system forms a disordered phase in bulk. (B) Spheres or cylinders of the lower surface energy blocks are formed. (C) Lamellae are formed. (D) Spheres or cylinders of the higher surface energy blocks are formed. The surface domains are drawn by speculation

† Institute for Materials Chemistry and Engineering.

* To whom correspondence should be addressed: Tel +81-3-3599-8311; Fax +81-3-3599-8166; e-mail yokoyama@ni.aist.go.jp.

10.1021/ma035191f CCC: $27.50
Published on Web 12/30/2003

strongly stretched. Therefore, architectures of block copolymers, i.e., *N* and *f*, are important factors for thickness of the surface domain and conformation of block copolymers which are related to hydrophobicity and its stability.

Typical fluorinated block copolymers which have been investigated are those with short (e.g., C_4F_9 to C_8F_{17}) fluorinated alkyl chains attached as side groups; therefore, they are "block−graft" copolymers that essentially differ from linear diblock copolymers. Those fluorinated polymers with fluoroalkyl side groups are expected to cover the surface with CF_3 groups with the lower critical surface tension than that of hydrocarbons and CF_2 groups. It has been found that the surface structures of such "block−graft" copolymers are strongly influenced by the structure of fluoroalkyl side groups.[9−18] Near-edge X-ray absorption fine structure (NEXAFS) studies have demonstrated that the surface properties of the fluorinated block copolymers are controlled by the orientation and packing of the side groups at the surface.[9,10,12,13,15,16] The fluoroalkyl side groups form a liquid crystal mesophase near the surface. They align in the direction of the surface normal or slightly tilt away from it, resembling self-assembled monolayers (SAMs) on substrates.

Although the primary structure of side groups is important for surface structure and property, the importance of block architectures, i.e., *N* and *f*, on the surface structure should not be overlooked. We have poorly understood how fluorinated block copolymers efficiently cover the surface with the fluoroalkyl side groups. A "graft" copolymer tends to lie parallel to the surface while a "block" copolymer prefers to orient perpendicular to the interface dividing the domains and to the surface when the interface and the surface are parallel each other such as the structure of lamellae at the surface.[7] We investigate how "block−graft" copolymers cover the surface and evaluate the influence of the architecture of the PS−PF copolymers on the structure of the surface domain and the conformation of the PS−PF copolymers.

We prepare a series of asymmetric block copolymers of poly[styrene-*block*-4-(perfluorooctylpropyloxy)styrene] (PS−PF) with the shorter PF block than the PS block. In the previous study[19] of this particular series of the PS−PF block copolymers, contact angles of dodecane as well as apparent surface fluorine concentrations of the PS−PF copolymers increased transitionally at a block fraction of 0.32. The transitional behavior at the particular block fraction has not been clearly understood. In this study, we analyze the surface segregation behavior of the series of the PS−PF block copolymers in detail and discuss the conformational change in the surface domain that causes the transitional behavior.

Experimental Section

Materials. A series of poly[styrene-*block*-4-(perfluorooctylpropyloxy)styrene] (PS−PF) block copolymers were polymerized by the following steps. First, polystyrenes were polymerized by *sec*-butyllithium as an initiator in tetrahydrofuran (THF) at −78 °C in high vacuum. The living polystyryllithium was subsequently reacted with 4-hydroxystyrene protected by *tert*-butyldimethylsilane (TBDMS) to form poly[styrene-*block*-4-(*tert*-butyldimethylsilyloxy)styrene] (PS−PSOTBDMS) followed by termination with methanol. PS−PSOTBDMS was deprotected in THF by adding hydrochloric acid to form poly(styrene-*block*-4-hydroxystyrene) (PS−PSOH). The Williamson reaction was used to introduce 1-bromo-3-perfluorooctylpropane into PSOH to obtain PS−PF copolymers. The chemical

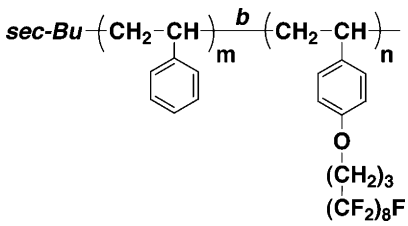

Figure 2. Chemical structure of the PS−PF block copolymers.

Table 1. Characteristics of PS−PF Block Copolymers

code	M_n/g mol^{-1}	f_{PF}^{wt}	code	M_n/g mol^{-1}	f_{PF}^{wt}
PSF75-09	75 000	0.09	PSF94-28	94 000	0.28
PSF27-25	27 000	0.25	PSF92-37	92 000	0.37
PSF34-28	34 000	0.28			

structures of the PS−PF copolymers are shown in Figure 2. The details of the synthesis, the polymerization, and the characterization have been described elsewhere.[19,20] The molecular weights of the PS blocks were measured by gel permeation chromatography (GPC) with PS standards. The weight fractions of the PF blocks, f_{PF}^{wt}, were measured by ^{1}H NMR, and the total molecular weights were calculated. The results of the characterization are listed in Table 1. The polydispersities of PS−PF copolymers are less than 1.1. The codes are PSF and the following two numbers: the first and second numbers indicate the total molecular weights in kg mol^{-1} and the weight fractions of PF blocks in percent, respectively. We use weight fractions instead of volume fractions due to lack of information about the density of the PF blocks. The volume fractions of those PF blocks are expected to be slightly lower than f_{PF}^{wt} since the density of fluorooctylpropane is about 1.6. ^{1}H NMR indicated that the ratio of the aromatic protons and the methylene protons adjacent to CF_2 agreed with the theoretical ratio, assuming perfect substitution within an experimental error. In addition, thin-layer chromatography with flame ionization detector found no remaining phenol group in the PS−PF block copolymers.

Sample Preparation. Specimens for X-ray photoelectron spectroscopy (XPS) and dynamic secondary ion mass spectrometry (SIMS) were prepared by spin-casting of toluene solutions of the PS−PF copolymers on silicon substrates of which surface were covered with native silicon oxide layers. The specimens were annealed at 180 °C in pressures less than 1×10^{-3} Pa for 24 h. The XPS spectra of the block copolymers are found to be almost the same after annealing of 8 h or longer at 180 °C, suggesting that equilibrium surface structures are formed, at most, in 8 h.

For SIMS analyses, sacrificial thin films of deuterated PS (dPS) (30−50 nm thick) were spun-cast, floated off onto distilled water, and picked up on top of the specimens. The deuterated PS is used so that the original surface is identified by the back edge of the dPS layer. This procedure also ensures that a steady-state sputtering condition is achieved before the SIMS sputtering crater reaches the original surface.

X-ray Photoelectron Spectrometry (XPS). Spectra were acquired on a PHI Quantum 2000 spectrometer equipped with a hemispherical capacitor analyzer using monochromated X-rays from Al Kα. A binding energy scale of the instrument was calibrated by setting Au $4f_{7/2}$ to 84.0 eV, Cu $2p_{3/2}$ to 932.6 eV, and Ag $3d_{5/2}$ to 368.3 eV. A chamber pressure during the measurements is maintained at $(1-4) \times 10^{-7}$ Pa. An X-ray beam operated at 20 W and focused to ca. 100 μm in diameter rastered over a 500 μm by 500 μm square area. We obtained sharp C 1s and F 1s peaks without neutralization for the thin films of PS−PF copolymers on silicon wafers used in this study: a small shift in binding energy was rescaled to 284.8 eV using the C 1s peak as a standard. Even without a neutralizer a loss of F 1s intensity against C 1s intensity was observed at a rate of 10% in 2 h with the X-ray beam power of 20 W. We limited an exposure time to 30 min for a spot irradiated by X-rays. An elemental survey scan from 0 to 1000

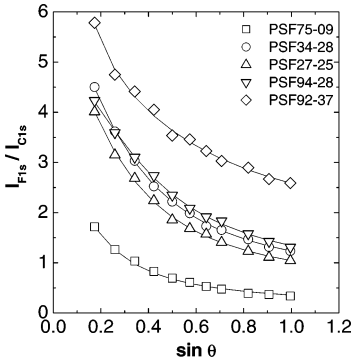

Figure 3. Angular dependences of the intensity ratios of F 1s and C 1s. The lines are the best fits of the model profiles in Figure 4 using eq 4.

eV with a pass energy of 100.5 eV was employed to check whether the surface was free from contamination. High-resolution scans of C 1s, F 1s, and O 1s regions were acquired with a pass energy of 35.8 eV at a takeoff angle, θ, which is the angle between the surface and the direction toward the analyzer. θ of 10, 15, 20, 25, 30, 35, 40, 45, 55, 65, and 85° are chosen for the angular dependence measurements. An analyzer aperture limited a range of takeoff angle to ±4°.

SIMS. Dynamic SIMS measurements were performed with an Atomica dynamic SIMS 4000 using a 4 keV, ca. 30 nA beam of O_2^+ ions at 45° off normal incidence, which was rastered over a 0.09 mm^2 region. The surface of each specimen was covered with a sacrificial layer of deuterated polystyrene (dPS) followed by evaporation of gold with a thickness of ca. 20 nm to reduce charge during the SIMS measurement. Charge neutralization using an electron flood gun was not employed. Negative ions of H, ^{2}H (D), C, CH, CD, F, and Si were monitored as a function of time from an electrically gated area that is less than 25% of the rastered area. Under such conditions, we obtained a depth profile with a Gaussian resolution of a full width at half-maximum of ca. 10 nm. A useful discussion of the important parameters for optimum dynamic SIMS depth profiling of polymers has been given by Schwarz et al.[21] By measuring the thickness of the polymer film using an ellipsometer, we convert a sputtering time into a depth assuming a steady rate of sputtering. Combining the depth scale with the known average chemical composition, we are able to convert the intensities of negative ions into the weight fraction of each block as a function of depth. The F^- signal is normalized to provide a depth profile of the PF block using

$$\Phi_{PF}^{wt}(z) = f_{PF}^{wt} z_0 I_{F^-}(z) / \int_0^{z_0} I_{F^-}(z)\, dz \qquad (1)$$

where z_0 and $I_{F^-}(z)$ are the film thickness and the F^- intensity at a depth z, respectively.

Results and Discussion

Surface Enrichment of Fluorine. The surface XPS analyses of the five PS−PF block copolymers with various M_n and f_{PF}^{wt} were performed as a function of a takeoff angle, θ. C 1s, O 1s, and F 1s peaks are identified by survey scans for all five samples. F 1s and O 1s show singlet symmetrical peaks at 689 and 533 eV, respectively. The intensities of F 1s and C 1s, I_{F1s} and I_{O1s}, are easily obtained by integration. C 1s shows two distinct peaks in the binding energy (BE) range between 283 and 296 eV depending on the electronic states. The entire C 1s region is integrated to define I_{C1s} for the following analysis. The ratio of intensities of F 1s and C 1s, I_{F1s}/I_{C1s}, is plotted in Figure 3 as a function of sin θ, which is proportional to the information depth. Apparent atomic fractions of fluorine, Φ_F^{app}, calculated from the values in Figure 3 at selected sin θ are listed in Table 2. Φ_F^{app} represents the integrated atomic fraction of fluorine near the surface. With increasing f_{PF}^{wt}, Φ_F^{app} increases monotonically at any selected angles in Table 2, whereas Φ_F^{app} with f_{PF}^{wt} of 0.25−0.28 shows no M_n dependence. It indicates qualitatively that f_{PF}^{wt} has stronger influence on Φ_F^{app} than M_n. This trend is in good accord with the previous study, in which contact angles of dodecane showed a strong dependence on the block fraction.[19] For all five samples, I_{F1s}/I_{C1s} monotonically decreases with sin θ, indicating that the concentrations of fluorine vary in the depth direction. The decreasing I_{F1s}/I_{C1s} with increasing sin θ has also been seen in the case of symmetric or PF-rich block copolymers in the literature.[5] The decay we observed, however, is much faster than that in the literature with increasing sin θ and hence suggests a thinner layer of fluorine with a thickness comparable to an inelastic mean free path (IMFP) of a photoelectron. A quantitative analyses of the XPS data and supplemental analyses by SIMS will be given in the following sections.

Table 2. Apparent Atomic Fractions of Fluorine (F) of PS−PF Block Copolymers, Φ_F^{app}, at Selected sin θ

		Φ_F^{app} at sin θ =		
code	f_{PF}^{wt}	0.17	0.50	1.00
PSF75-09	0.09	0.35	0.17	0.11
PSF34-28	0.28	0.59	0.42	0.27
PSF27-25	0.25	0.56	0.37	0.26
PSF94-28	0.28	0.57	0.42	0.28
PSF92-37	0.37	0.65	0.52	0.45

Surface Structures of Fluorinated Blocks. An XPS intensity from a depth, z, decays exponentially due to an inelastic scattering process with a decay rate called electron escape depth, λ_i; therefore, the XPS intensities are given by the Laplace transform of an atomic fraction, $\Phi_i(z)$, of an element i.

$$I_i(\lambda_i) = T\frac{I_i^\circ}{\lambda_i}\int_0^\infty \Phi_i(z) e^{-z/\lambda_i}\, dz \equiv L[\Phi(z)] \qquad (2)$$

T is an unknown transmission efficiency of the analyzer depending on geometry of the specimen, an incident X-ray beam, and an analyzer. The electron escape depth, λ_i, of an element, i, is given by

$$\lambda_i = \lambda_i^\circ \sin\theta \qquad (3)$$

where λ_i° is IMFP of the element i. On the basis of the kinetic energy dependence of IMFP proposed by Ashley,[22] λ_{C1s}° and λ_{F1s}° are 3.8 and 2.8 nm, respectively, for the incident X-ray energy of Al Kα. The atomic sensitivity factors given by the manufacturer for C 1s, I_{C1s}°,, and for F 1s, I_{F1s}°, are 0.314 and 1.000, respectively. By taking the intensity ratio of F 1s and C 1s simultaneously measured at the same angle, T, is canceled, and then the intensity ratio can simply be written by

$$\frac{I_{F1s}}{I_{C1s}} = \frac{I_{F1s}^\circ/I_{C1s}^\circ}{\lambda_{F1s}/\lambda_{C1s}} \frac{\int_0^\infty \Phi_{F1s}(z) e^{-z/\lambda_{F1s}}\, dz}{\int_0^\infty \Phi_{C1s}(z) e^{-z/\lambda_{C1s}}\, dz} \qquad (4)$$

In general, the inverse Laplace transform of the equation, $L^{-1}[I_i(\lambda_i)]$, cannot be found analytically. Hence, the depth profiles near the surface are numerically computed by the following procedure. (1) Assume a model

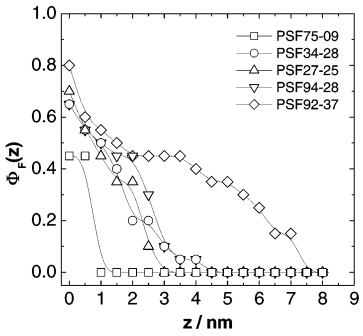

Figure 4. Model depth profiles of atomic fractions, $\Phi_F(z)$, used to fit the angular dependences of the intensity ratios of F 1s and C 1s. The presence of hydrogen is neglected for the definition of $\Phi_F(z)$. The lines are guides for the eye. The theoretical fluorine fractions, Φ_F, of CF_3, C_8F_{17}, and PF are 0.75, 0.68, and 0.47, respectively.

depth profile. (2) Calculate a relative intensity, I_{F1s}/I_{C1s}, using eq 4. (3) Fit the calculated I_{F1s}/I_{C1s} with the measured I_{F1s}/I_{C1s} and obtain the sum of the mean-square difference $\sum\chi^2$. (4) Accept the model when $e^{-\Delta(\sum\chi^2)} > W$, where $\Delta(\sum\chi^2)$ is the difference of current $\sum\chi^2$ from previous $\sum\chi^2$ and W is a weighting factor. The weighting factor is an arbitrary number controlling a conversion of the iteration loop. Repeat the step from (1) through (4) until the best fit is achieved. The model profile $\Phi_F(z)$ takes a value from 0 to 1 with an increment of 0.05, where z takes a value from 0 to 10 nm with an increment of 0.5 nm. The models fit the I_{F1s}/I_{C1s} very well as indicated by the lines in Figure 3. The model profiles used to fit the data, $\Phi_F(z)$, are plotted against z in Figure 4. The presence of hydrogen is neglected in the definition of the atomic fraction. The same final profile was obtained by this procedure regardless of an arbitrary choice of an initial profile.

First, we compare PSF27-25, PSF34-28, and PSF94-28 with nearly the same f_{PF}^{wt} but with different M_n. If those copolymers form half of a lamella near the surface, which is occasionally observed even for an asymmetric block copolymer near an attractive solid wall,[23−25] the PF domain thicknesses of those copolymers should depend on the molecular weights. In the case of a lamellar structure, a block copolymer chain tends to orient perpendicular to the interface between the domains and to be stretched to avoid undesired contact between the blocks especially in strong segregation.[7] A lamellar thickness, D, has a molecular weight dependence $D \sim M_n^{\nu}$, where ν is an exponent greater than 0.5. The exponent should be at least 0.5 even in weak segregation limit.[7] As seen in Figure 4, the surface domain thickness of PF block shows no correlation on the overall molecular weight, which contradicts the observation for lamellar forming block copolymers. This lack of molecular weight dependence indicates that the backbone of the PF block is lying down parallel to the surface. A similar surface structure has been suggested for a graft copolymer with short hydrophobic side groups,[26] where the backbone of the graft copolymer lies parallel to the surface and orients the side groups perpendicular to the surface. The surface is covered by a monolayer of the PF block lying down parallel to the surface and orienting the side group perpendicular to the surface, similar to the surface structure of graft copolymer,[26] followed by the PS block dangling down from the surface monolayer of the PF block. Another evidence of the proposed structure is that $\Phi_F(z)$ in the region of 0−1.5 nm is greater than the average fluorine fraction of PF, where the theoretical fluorine fraction, Φ_F, of CF_3, C_8F_{17}, and PF are 0.75, 0.68, and 0.47, respectively. The exclusion of the PF backbone from the top surface region within 1.5 nm from the surface is clearly observed. Since the length of C_8F_{17} is ca. 1.2 nm, these three copolymers have the surface domain of the nearly saturated C_8F_{17} side groups orienting perpendicular to the surface with an approximate thickness of 1.5 nm followed by almost no PF block domain. We can at least claim that the backbone is excluded from the top surface region if the surface is not fully packed with the C_8F_{17} side groups. A schematic picture of the surface structure of those three PS−PF block copolymers is shown in Figure 5B. The thick rigid rods indicate the C_8F_{17} side groups attached to the backbone. The large circles are the joints between the PF and PS blocks. The graph on the right-hand side is the depth profile of fluorine expected from the picture on the left-hand side. The expected depth profiles are consistent with the measured depth profiles in Figure 4. The more detailed analysis of the local structure of the fluorooctyl side group will be given in the following section in order to prove that the C_8F_{17} side groups are orienting toward the surface.

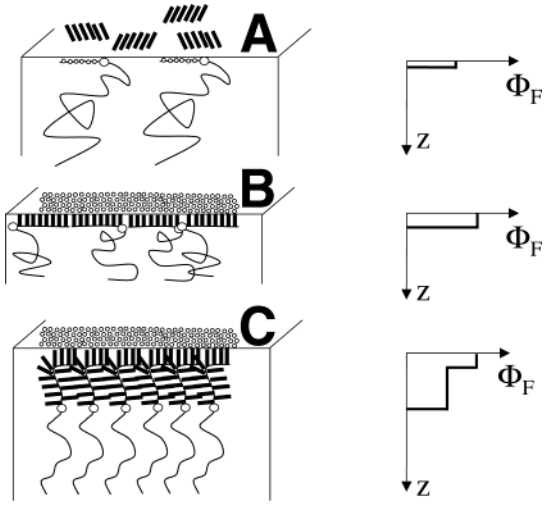

Figure 5. Schematic pictures of chain conformations consistent with the depth profiles of atomic fractions in Figure 4. The flexible chains and the short solid lines represent PS blocks and C_8F_{17} side groups, respectively. (A) $f_{PF}^{wt} = 0.1$. The side groups are lying down on the surface. (B) $f_{PF}^{wt} = 0.25-0.28$. The side groups are standing toward the surface while the backbone of the PF block is lying parallel to the surface. (C) $f_{PF}^{wt} = 0.37$. The backbone of the PF block is orienting perpendicular to the surface while the side groups and the backbone lie perpendicular and parallel to the surface, respectively, only in the top surface region (0−1.5 nm).

PSF92-37, on the other hand, shows a significantly different depth profile. $\Phi_F(z)$ of PSF92-37 with f_{PF}^{wt} of 0.37 in the top surface region from 0 to 1.5 nm in depth is similar to those of three block copolymers with f_{PF}^{wt} of 0.25−0.28; however, $\Phi_F(z)$ of PSF92-37 in a range of depth from 1.5 to 8 nm is substantially higher. We have shown by comparing PSF94-28 and PSF92-37 that the small increment of f_{PF}^{wt} from 0.28 to 0.37 with the same M_n makes the drastic difference in Φ_F^{app} in Table 2; nonetheless, the top surfaces regions from 0 to 1.5 nm in depth are almost the same as seen in Figure 4. The surface is covered by the PF block with the C_8F_{17} side group orienting toward the surface similar to the

structure in Figure 5B; however, the thickness of the surface PF domain is much thicker. The PF block is not parallel to the surface; furthermore, the joint between the PF and PS blocks is about 6 nm away from the surface, and the vector from the joint between PF and PS to the chain end of the PF block is pointing toward the surface similar to an ordinary lamellar structure of block copolymers, in contrast to the Figure 5B where the vector is parallel to the surface. A possible chain conformation of PSF92-37 is schematically shown in Figure 5C. The vector that characterizes the orientation of the PF block of PSF92-37 stands more vertically, resulting in the much thicker surface domain. It should be noted that the plateau of $\Phi_F(z)$ of 0.4−0.5 can be found underneath the surface monolayer of the C_8F_{17} side groups in Figure 4. This region corresponds to a domain of the whole PF blocks with Φ_F of 0.46 successively connected to the surface monolayer of the C_8F_{17} side groups as schematically shown in Figure 5C. Graft copolymers with fluoroalkyl side group form smectic layers parallel to the surface.[26] If such smectic multiple layers of the C_8F_{17} side groups parallel to the surface existed at the surface, the PS block would pass through such layers experiencing unfavorable contacts. Therefore, it is unlikely for the PSF92-37 copolymer to form the smectic multiple layers with all the side groups orienting perpendicular to the surface. When the vector is pointing to the surface, the fluoroalkyl side groups tend to be perpendicular to the vector and parallel to the dividing interface between the PF and PS domains. This is a general trend of side-chain liquid-crystal (LC) mesogens in block copolymers to satisfy the homogeneous boundary condition of the mesogens.[27] The structure in Figure 5C is drawn so that the two opposite demands are satisfied. The surface monolayer of the C_8F_{17} side groups must be somehow connected to the PF domain underneath the layer. The C_8F_{17} side groups flip the orientation and may have some distortion to maintain the connectivity. At f_{PF}^{wt} of ca. 0.3 a half lamella at the surface becomes stable while the top surface is still covered by the orienting C_8F_{17} side groups controlled by the lowest surface energy of CF_3. This structural change at this f_{PF}^{wt} apparently causes the sudden jump of the contact angles of dodecane and the apparent surface fluorine concentration in the previous study.[19] Further evidence of the C_8F_{17} side groups in the top surface region standing nearly perpendicular to the surface will be given in the following section.

PSF75-09 with f_{PF}^{wt} of 0.09 shows a remarkably different behavior from the other PS−PF copolymers. By the model fitting, we find that the thickness of the surface domain is not only thinner than the other copolymers but also even thinner than the length of the C_8F_{17} side group. In addition the surface is not fully saturated with the C_8F_{17} side group with Φ_F of 0.68. The asymmetry of PSF75-09 prevents the PF block from segregating to the surface by an entropic penalty of stretching in the PS block. As shown in Figure 5A, the C_8F_{17} side group of PSF75-09 may lie down on the surface as well as the backbone of PF to cover the surface as much as possible with the limited number of the C_8F_{17} side groups. The suggested structure is in contrast to the other block copolymers of which the C_8F_{17} side groups in the top surface region are closely packed and oriented toward the surface. There is a possibility that the C_8F_{17} side groups form surface aggregates to cover the surface partially. We have tried to detect the surface inhomogeneity by scanning force microscopy, but no clear evidence of such aggregates was found. A study of surface segregation of fluorinated alkyl at the chain end of polystyrenes, which is an extreme case of an insufficient supply of fluoroalkyl groups to the surface, also suggests that the segregated fluoroalkyl groups lie parallel to the surface[28] similar to our experimental results for PSF75-09. Although additional analysis is necessary for the confirmation of such surface structure, a small quantity of surface segregates makes the further analysis difficult.

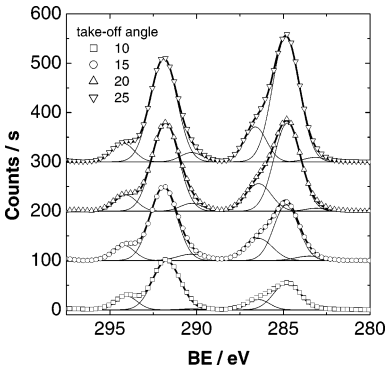

Figure 6. Chemical shifts of C 1s photoelectrons form the surface of PSF94-28 and its dependence on the takeoff angle.

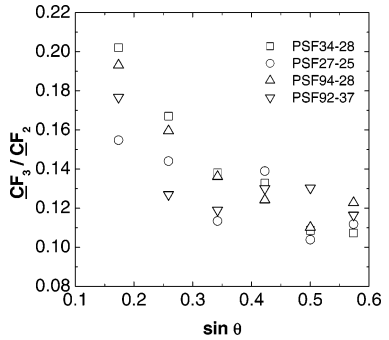

Figure 7. Angular dependences of the ratios of the atomic fractions of the CF_3 group over that of the CF_2 group of the PS−PF copolymers.

Table 3. Binding Energies of C 1s Regions and Assignments

functional group	binding energy/eV
CF_3	293.9
CF_2	291.6
C−O and C−CF_2	286.0
hydrocarbon (reference)	284.8

Structures of Fluorinated Side Group. A chemical shift of C 1s peak contains more specific information about a location of a chemical group. In particular the C 1s peaks of CF_2 and CF_3 groups can be distinguished. We introduced four Gauss−Lorentz (GL) functions to fit the C 1s region with peak assignments given in Table 3.[29] Examples of the data fitting are shown in Figure 6. The data are shifted vertically by 100 counts to compare the spectra taken at different takeoff angles.

The ratios of the peak areas of CF_3 at 294 eV over CF_2 at 292 eV obtained by peak fitting are plotted as a function of sin θ. PSF75-09 is excluded from this analysis since the intensity of CF_3 was too low to be fit, and the $\pi \rightarrow \pi^*$ shake-up peak is not negligible even at low sin θ. For the other block copolymers, the ratios CF_3/CF_2 are compared in Figure 7 in the region of $0 < \sin\theta$

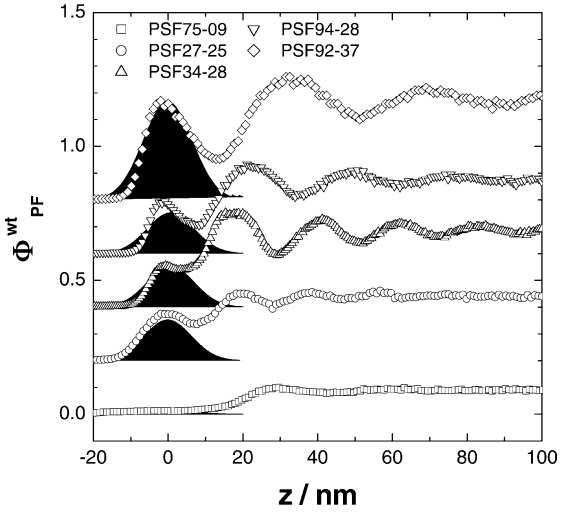

Figure 8. SIMS depth profiles of the PS−PF copolymers. The peak at $z = 0$ corresponds to the surface domain. The weight fractions of the PF blocks, f^{wt}_{PF}, are shifted by 0.2 for clarity. The shadowed areas are the surface domain profiles expected from convolutions of the surface domain depth profiles obtained by XPS and an instrumental resolution function.

< 0.6 where the influence of the $\pi \rightarrow \pi^*$ shake-up peak is negligible.

Considering the error for this analysis is 10−15%, we find the trend of decreasing CF_3/CF_2 ratio with increasing takeoff angle. This decay of the ratio of CF_3 over CF_2 shown in Figure 7 clearly indicates that the CF_3 groups are enriched at the surface compared to the CF_2 groups. The enrichment of the CF_3 groups is driven by the lowest critical surface tension of CF_3 in the copolymer and the packing of C_8F_{17} side groups at the surface. This trend supports the picture schematically shown in Figure 5 and agrees with the results of similar fluorinated block copolymers in the references.[9,10,15]

Marginal Region between Surface and Bulk. Although XPS has successfully constructed the real space depth profiles using the method described above, the length scale totally relies on IMFP of F 1s and C 1s calculated by theory.[22] We employ an independent measurement of depth profiles of the PF block using dynamic SIMS. Although SIMS has limited resolution in depth scale, ca. 10 nm of fwhm, the amount of fluorine at the surface can still be determined. In addition, SIMS can detect internal layered structures, if exist, as well as the surface domain. Converted SIMS depth profiles of the PS−PF block copolymers are shown in Figure 8. The depth profiles are shifted vertically by 0.2 for clarity. The shadowed areas correspond to the profiles obtained by convolutions of the surface PF domains in Figure 4 with a experimental Gaussian resolution function with a full width at half-maximum ca. 10 nm. Reasonable agreements are found in Figure 8. Thus, the depth profiles obtained by XPS in Figure 4 are quantitatively correct as supported by the SIMS analysis, which is the independent method that does not rely on IMFP.

In addition to supporting the validity of IMFP in XPS analysis, the SIMS depth profiles show internal layered structures often found in ordered structures near the surface. In Figure 8, the oscillations due to the layering of the PF domains have maxima next to the surface domains and decay with depth. Layered structures can be observed in either a lamellar, cylinder, or spherical structure. Lamellae[30−35] and cylinders[23] orient parallel to the surface at equilibrium, giving a periodic layered structure normal to the surface. Even spherical domains show a periodic layered structure in which (110) plane of the body-centered-cubic (bcc) structure is parallel to the surface.[24,25] The decay of these periodic oscillations of the PF block fraction is indicative of either a kinetically trapped inequilibrium structure or disordered bulk structure, which will be discussed in the Appendix.

For PSF75-09, no ordered structure is observed except near the surface region. This block copolymer may be identified to be in a disordered phase. Although SIMS cannot distinguish between a homogeneous mixture and randomly oriented domains, a periodic oscillation should be induced by the surface if ordered domains exist. Only a small surface domain peak is expected from XPS analysis which is consistent with the SIMS depth profile. You may notice that Φ^{wt}_{PF} seems to start rising at 20 nm from the surface. Although the surface is covered by a very small amount of the PF block, a 10 times greater amount of the PS block has to follow due to its high asymmetry and conservation of mass per molecule. In addition, if the PF internal domains exist, the domains are surrounded by thick PS domains. Therefore, the region from 0 to 20 nm from the surface is mostly occupied by the PS blocks with an extremely thin and almost invisible layer of the PF block at the surface, which cannot be observed by SIMS due to its limited resolution but has been detected by XPS.

For PSF27-25, PSF34-28, and PSF94-28, the surface domain structures revealed by XPS and SIMS are almost the same; however, the periodicity and amplitude of internal structures are dependent on the total molecular weights, and hence the differences in the sizes of the bulk order structures are evident. PSF27-25 has the smallest periodicity and PSF94-28 has the largest periodicity, which are consistent with their molecular weights. It should be emphasized that the surface structure of block copolymers can be unique due to geological requirements, surface tensions, and local structures such as structures of side groups.

Conclusions

The C_8F_{17} side groups of the PS−PF block copolymers may lie down on the surface and cover the surface partially when f^{wt}_{PF} is about 0.1 as suggested by the measured thickness of the surface PF domain thinner than the length of the C_8F_{17} side group. As f^{wt}_{PF} increases to 0.25−0.28, the C_8F_{17} side groups of the PF block lie perpendicular to the surface to form a monolayer of the C_8F_{17} side groups, and the backbone becomes parallel to the surface. As f^{wt}_{PF} further increases to 0.37, the PF domain becomes thicker while the top surface structure of the C_8F_{17} side groups is still unchanged. The crossover from the monolayer regime to the thick lamella-like regime occurs around $f^{wt}_{PF} \simeq 0.3$. With increasing f^{wt}_{PF}, the surface structure similar to half of a lamella becomes stable and the backbone of the PF likes to stand perpendicular to the interface between the PS and PF domains and the surface. The structural change occurs around f^{wt}_{PF} of 0.3, at which the sudden changes in the contact angle of dodecane and the apparent fluorine concentration have been reported.[19] The origin of this crossover is related to the "block−graft" architecture of the PS−PF copolymers: a graft copolymer prefers side groups pointing up to the

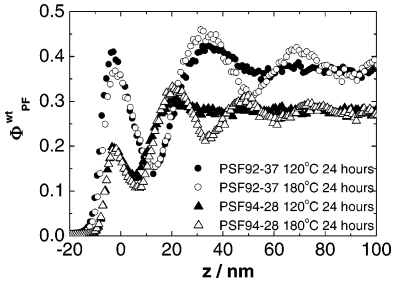

Figure 9. Temperature dependence of the structure development underneath the surface domain. The oscillations propagate from the surface domain to the bulk.

surface with a backbone lying down parallel to the surface while a block copolymer generally favors a backbone orienting perpendicular to the interface and the surface.

Acknowledgment. This research has been partially funded by the Nanostructure Polymer Project by the New Energy and Industrial Technology Development Organization (NEDO). A part of this work was supported by "Nanotechnology Support Project" of the Ministry of Education, Culture, Sports, Science and Technology (MEXT), Japan.

Appendix

Inequilibrium Structure or Disorder. Depth profiling techniques, in general, cannot distinguish between an inequilibrium structure without any orientation and a disordered structure. All the specimens used for XPS and SIMS analysis were annealed at 180 °C for 24 h. We found that the XPS spectra of the PS−PF block copolymers annealed at 180 °C for 8 and 24 h are within experimental error; therefore, the surface domains are in equilibrium. The decaying oscillation of depth profile obtained by SIMS is due to either a kinetically trapped inequilibrium structure or a fluctuating disordered structure perturbed by the surface. In particular, for those with larger M_n and f_{PF}, it takes an extremely long time to reach equilibrium due to their slow diffusion decelerated by thermodynamic barrier of the ordered domain.[36]

If the structure is in kinetically trapped inequilibrium, the layered structure develops less at reduced temperature. However, if it is in a disordered phase perturbed by the surface, reducing temperature enhances the growth of the layered structure. PSF94-28 and PSF92-37 are annealed at 120 and 180 °C for 24 h. The results of the SIMS analysis are shown in Figure 9. In Figure 9, we find that the surface domain is independent of the annealing temperature; however, the internal periodic layered structure is growing farther at the elevated temperature. This trend indicates that the layered structure is induced at the surface, but the propagation process is kinetically limited.

References and Notes

(1) Katano, Y.; Tomono, H.; Nakajima, T. *Macromolecules* **1994**, *27*, 2342.
(2) Hapken, J.; Möller, M. *Macromolecules* **1992**, *25*, 1461.
(3) Schneider, J.; Erdelen, C.; Ringsdorf, H.; Rabolt, J. F. *Macromolecules* **1989**, *22*, 3475.
(4) Rabolt, J. F.; Russell, T. P.; Tweig, R. J. *Macromolecules* **1984**, *17*, 2786.
(5) Kassis, C. M.; Steehler, J. K.; Betts, D. E.; Guan, Z.; Romack, T. J.; DeSimone, J. M.; Linton, R. W. *Macromolecules* **1996**, *29*, 3247.
(6) Bottino, F. A.; Di Pasguale, G.; Pollicino, A.; Pilati, F.; Toselli, M.; Tonelli, C. *Macromolecules* **1998**, *31*, 7814.
(7) Bates, F. S.; Fredrickson, G. H. In *Thermoplastic Elastomers*, 2nd ed.; Hanser Publishers: New York, 1998; Chapter 12, p 336.
(8) Leibler, L. *Macromolecules* **1980**, *13*, 1602.
(9) Genzer, J.; Sivaniah, E.; Kramer, E. J.; Wang, J.; Körner, H.; Xiang, M.; Char, K.; Ober, C. K.; DeKoven, B. M.; Bubeck, R. A.; Chaudhury, M. K.; Sambasivan, S.; Fisher, D. A. *Macromolecules* **2000**, *33*, 1882.
(10) Genzer, J.; Sivaniah, E.; Kramer, E. J.; Wang, J.; Körner, H.; Char, K.; Ober, C. K.; DeKoven, B. M.; Bubeck, R. A.; Fisher, D. A.; Sambasivan, S. *Langmuir* **2000**, *16*, 1993.
(11) Sivaniah, E.; Genzer, J.; Fredrickson, G. H.; Kramer, E. J.; Xiang, M.; Li, X.; Ober, C. K.; Magonov, S. *Langmuir* **2001**, *17*, 4342.
(12) Hayakawa, T.; Wang, J.; Xiang, M.; Li, X.; Ueda, M.; Ober, C. K.; Genzer, J.; Sivaniah, E.; Kramer, E. J.; Fisher, D. A. *Macromolecules* **2000**, *33*, 8012.
(13) Xiang, M.; Li, X.; Ober, C. K.; Char, K.; Genzer, J.; Sivaniah, E.; Kramer, E. J.; Fischer, D. A. *Macromolecules* **2000**, *33*, 6106.
(14) Wang, J.; Mao, G.; Ober, C. K.; Kramer, E. J. *Macromolecules* **1997**, *30*, 1906.
(15) Genzer, J.; Sivaniah, E.; Kramer, E. J.; Wang, J.; Xiang, M.; Char, K.; Ober, C. K.; Bubeck, R. A.; Fischer, D. A.; Graupe, M.; Colorado, R., Jr.; Shmakova, O. E.; Lee, T. R. *Macromolecules* **2000**, *33*, 6068.
(16) Li, X.; Andruzzi, L.; Chiellini, E.; Galli, G.; Ober, C. K.; Hexemer, A.; Kramer, E. J.; Fischer, D. A. *Macromolecules* **2002**, *35*, 8078.
(17) Iyengar, D. R.; Perutz, S. M.; Dai, C.-A.; Ober, C. K.; Kramer, E. J. *Macromolecules* **1996**, *29*, 1229.
(18) Perutz, S.; Wang, J.; Kramer, E. J.; Ober, C. K.; Ellis, K. *Macromolecules* **1998**, *31*, 4272.
(19) Sugiyama, K.; Nemoto, T.; Koide, G.; Hirao, A. *Macromol. Symp.* **2002**, *181*, 135.
(20) Hirao, A.; Koide, G.; Sugiyama, K. *Macromolecules* **2002**, *35*, 7642.
(21) Schwarz, S. A.; Wilkens, B. J.; Pudensi, M. A. A.; Rafailovich, M. H.; Sokolov, J.; Zhao, X.; Zhao, W.; Zheng, X.; Russel, T. P.; Jones, R. A. L. *Mol. Phys.* **1992**, *76*, 937.
(22) Ashley, J. C. *J. Electron Spectrosc. Relat. Phenom.* **1982**, *28*, 177.
(23) Liu, Y.; Zhao, W.; Zheng, X.; King, A.; Singh, A.; Rafailovich, M. H.; Sokolov, J.; Dai, K. H.; Kramer, E. J.; Schwarz, S. A.; Gebizlioglu, O.; Sinha, S. K. *Macromolecules* **1994**, *27*, 4000.
(24) Yokoyama, H.; Kramer, E. J.; Rafailovich, M. H.; Sokolov, J.; Schwarz, S. A. *Macromolecules* **1998**, *31*, 8826.
(25) Yokoyama, H.; Mates, T. E.; Kramer, E. J. *Macromolecules* **2000**, *33*, 1888.
(26) Sheiko, S.; Lermann, E.; Möller, M. *Langmuir* **1996**, *12*, 4015.
(27) Mao, G.; Wang, J.; Clingman, S. R.; Ober, C. K.; Chen, J. T.; Thomas, E. L. *Macromolecules* **1997**, *30*, 2556.
(28) Tanaka, K.; Kawaguchi, D.; Yokoe, Y.; Kajiyama, T. Takahara, A.; Tasaki, S. *Polymer* **2003**, *44*, 4171.
(29) It is necessary to have two more GL functions other than the peaks in Table 3 to fit the low binding energy sides of CF_2 and hydrocarbon peaks as seen in Figure 6. A similar problem with assigning peaks for fluorinated block copolymers has also been reported.[5] We are not able to identify the reason for the additional peaks in low binding energy side necessary to fit the data; however, those peaks in this study are much smaller than those found in the literature.[5] Hence, we simply add the area to either the adjacent CF_2 or hydrocarbon peak for further analysis.
(30) Fredrickson, G. H. *Macromolecules* **1987**, *20*, 2859.
(31) Anastasiadis, S. H.; Russell, T. P.; Satija, S. K.; Majkrzak, C. F. *Phys. Rev. Lett.* **1989**, *62*, 1852.
(32) Menelle. A.; Russell, T. P.; Anastasiadis, S. H.; Satija, S. K.; Majkrzak, C. F. *Phys. Rev. Lett.* **1992**, *68*, 67.
(33) Coulon, G.; Russell, T. P.; Deline, V. R.; Green, P. F. *Macromolecules* **1989**, *22*, 2581.
(34) Russell, T. P.; Coulon, G.; Deline, V. R.; Miller, D. C. *Macromolecules* **1989**, *22*, 4600.
(35) Foster, M. D.; Sikka, M.; Singh, N.; Bates, F. S.; Satija, S. K.; Majkrzak, C. F. *J. Chem. Phys.* **1992**, *96*, 8605.
(36) Yokoyama, H.; Kramer, E. J. *Macromolecules* **1998**, *31*, 7871.

MA035191F